Strategy to suppress epidemic explosion in heterogeneous metapopulation networks

Chuansheng Shen,[1,2] Hanshuang Chen,[3] and Zhonghuai Hou[1,*]

[1]*Hefei National Laboratory for Physical Sciences at Microscales and Department of Chemical Physics, University of Science and Technology of China, Hefei 230026, China*

[2]*Department of Physics, Anqing Teachers College, Anqing 246011, China*

[3]*School of Physics and Material Science, Anhui University, Hefei 230039, China*

(Received 2 March 2012; revised manuscript received 26 July 2012; published 24 September 2012)

We propose an efficient strategy to suppress epidemic explosion in heterogeneous metapopulation networks, wherein each node represents a subpopulation with any number of individuals and is assigned a curing rate that is proportional to k^{α} with the node degree k and an adjustable parameter α. We perform stochastic simulations of the dynamical reaction-diffusion processes associated with the susceptible-infected-susceptible model in scale-free networks. We find that the epidemic threshold reaches a maximum when α is tuned at $\alpha_{\rm opt} \simeq 1.3$. This nontrivial phenomenon is robust to the change of the network size and the average degree. In addition, we carry out a mean field analysis to further validate our scheme, which also demonstrates that epidemic explosion follows different routes for α larger or less than $\alpha_{\rm opt}$. Our work suggests that in order to efficiently suppress epidemic spreading on heterogeneous complex networks, subpopulations with higher degrees should be allocated more resources than just being linearly dependent on k.

DOI: 10.1103/PhysRevE.86.036114 PACS number(s): 89.75.Hc, 89.20.−a, 89.75.Fb, 87.23.Ge

I. INTRODUCTION

In the lasttwo decades, we have witnessed dramatic advances in complex network research, which has been one of the most active topics in statistical physics and closely related disciplines [1–3]. The central issue in this field is to study how the network topology influences the dynamics [4–6]. As one of the typical dynamical processes built on complex networks, epidemic spreading has attracted significant attention [7–24].

Recently, metapopulation dynamics on heterogeneous networks, which incorporates mobility over the nodes, local interaction at the nodes, and a complex network structure, has gained great research attention [24–42]. In this context, reaction-diffusion (RD) processes have been widely used to model phenomena as diverse as the spread of epidemics and computer viruses [24–30], biological pattern formation [31,32], chemical reactions [33–35], population evolution [36], and many other spatially distributed systems [37–40]. In a series of important papers, Colizza *et al*. [25] provided an analysis of the basic RD process of a paradigmatic epidemic model, the susceptible-infected-susceptible (SIS) model, defined on heterogeneous metapopulation networks. Therein, each network node represents an urban area together with its population, and edges represent air travel fluxes along which individuals diffuse, coupling the epidemic spreading in different urban areas. They paid particular attention to the epidemic threshold ρ_c and found that ρ_c is strongly affected by the topological fluctuations of the network for diffusing susceptible individuals. Later, Balcan and Vespignani [40] extended such analysis to non-Markovian diffusive processes on complex networks, wherein individuals have a memory of their location of origin and displaced individuals return to their original subpopulation with a certain rate. Very recently, Vespignani [41] reviewed and highlighted some of the recent progresses in modeling dynamic processes that integrates the complex features and heterogeneities of real-world systems. Nevertheless, all the studies so far have treated the curing rate μ as a homogenous parameter; that is, it is not dependent on the local property of the network node, such as the degree k. Note, however, in reality the curing rate should certainly be associated with the available medical resources in the local subpopulation, and thus it is reasonable to assume that μ is a function of the degree k. It is therefore interesting to ask how the metapopulation dynamics of the SIS model, for instance, the epidemic threshold ρ_c, would depend on such a k-dependent curing strategy. The answer to this question may provide useful instructions regarding the control of epidemic explosion in metapopulation networks.

In the present paper, we have addressed such a question by considering a simple strategy, $\mu_k \sim k^{\alpha}$, where k denotes the node degree and α is an adjustable parameter. If $\alpha = 0$, one recovers the usual cases studied in previous works. Herein, we mainly focus on the influence of varying α on the value of ρ_c. Interestingly, we found that ρ_c bypasses a clear-cut maximum at a certain $\alpha_{\rm opt}$, which corresponds to an optimal strategy to suppress epidemic explosion. This observation along with the value of $\alpha_{\rm opt}$ is robust to the change of the network size and the average network degree. To place the finding on a solid foundation, we have also performed a mean field (MF) analysis, wherein ρ_c is identified as the onset point where the global healthy state with no infected individuals loses stability. The MF equations successfully reproduce the $\rho_c \sim \alpha$ dependences and also provide more insights regarding the routes to epidemic explosion for different values of α.

II. MODEL DESCRIPTION

We consider a system of N distinct subpopulations, each corresponding to a network node. Individuals inside each node run stochastically through the paradigmatic SIS model [43–45]. Schematically, the stochastic infection dynamics is

*hzhlj@ustc.edu.cn

given by

$$S + I \xrightarrow{\beta} 2I, \quad I \xrightarrow{\mu_k} S. \tag{1}$$

The first reaction reflects the fact that each susceptible (S) individual becomes infected upon encountering one infected (I) individual at a probability rate β. The second one indicates that infected individuals are cured and become again susceptible at a k-dependent rate μ_k. Inside each network node, reaction processes take place under the assumption of a homogenous mixing. After the reaction, individuals randomly diffuse along the edges to neighboring nodes.

In this model, a significant and general result is that the system undergoes an absorbing-state phase transition with increasing density ρ, in analogy with critical phenomena [6]. Here ρ is defined as the total number of individuals divided by N. The critical density ρ_c indicates the epidemic threshold.

To begin, we perform our strategy on scale-free (SF) networks by using the Barabási-Albert (BA) model [46] with power-law degree distribution $p(k) \sim k^{-3}$. Scale-free networks are much more heterogeneous and serve as better candidates to test our strategy than other homogeneous networks, such as small-world or random networks. For a node i with degree k_i, the curing rate is given by

$$\mu_{k_i} = \frac{k_i^{\alpha}}{\sum_j k_j^{\alpha}/N}. \tag{2}$$

Herein, μ_{k_i} is normalized such that the average curing rate remains constant: $\bar{\mu} = \frac{1}{N}\sum_i \mu_{k_i} = 1$. Note that in other related works about epidemic dynamics on networks, a k-dependent strategy, but associated with the infection rate β, had also been considered [17,47].

The system evolves in time according to the following rules [25]: The dynamics proceeds in parallel and follows a discrete time step representing the fixed time scale τ of the process. The reaction and diffusion rates therefore are converted into probabilities. At each time step, the system is updated as follows. Inside each network node with degree k, each infected individual is cured with probability $\mu_k\tau$. At the same time, each susceptible individual becomes infected with probability $1-(1-\beta\tau)^{n_I}$, where n_I is the total number of infected individuals in the node. After all nodes have been updated for the reactions, diffusion processes take place by allowing each individual to move into a randomly chosen neighboring node with probability $D_I\tau$ and $D_S\tau$, for infected and susceptible individuals respectively, where $D_I(D_S)$ denotes the corresponding diffusion constant. In our simulation, the parameters are $N = 1000$, $\beta = 0.5$, $D_I = D_S = 1.0$, and $\tau = 0.001$ if not otherwise specified. Each simulation plot is obtained via averaging over 20 independent runs.

III. SIMULATION RESULTS

Figure 1(a) shows how the proportion ρ_I/ρ, where $\rho_I = \sum n_I/N$ denotes the density of infected individuals in the whole network, increases with ρ for four different values of α. Clearly, the system undergoes a phase transition at a certain threshold density ρ_c, above which ρ_I/ρ monotonically increases from zero. For $\rho < \rho_c$, the system stays in a "healthy" state with $\rho_I = 0$. Interestingly, ρ_c reaches a largest

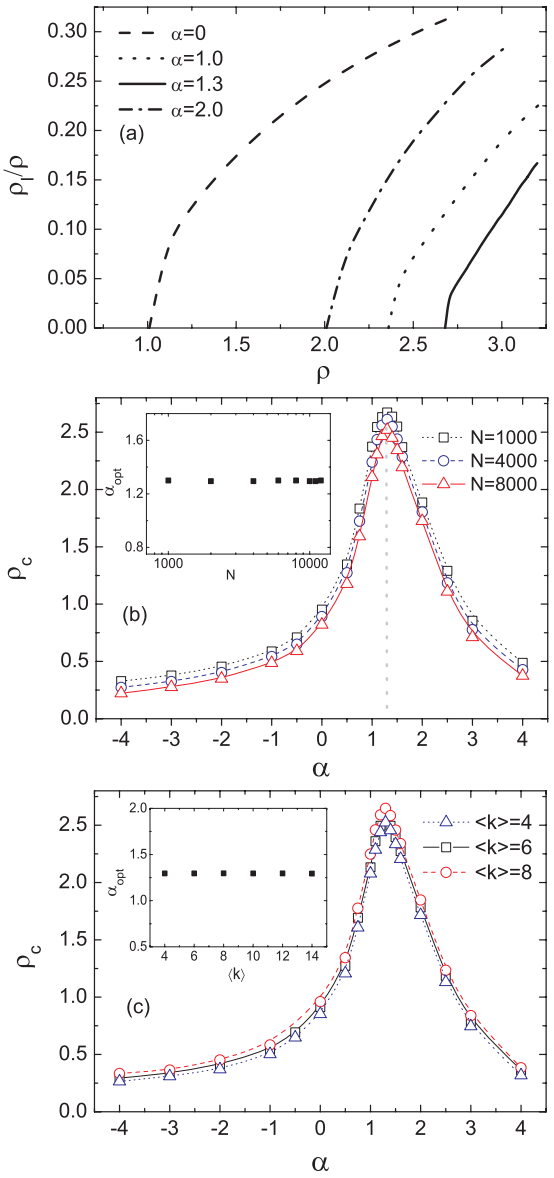

FIG. 1. (Color online) (a) The proportion ρ_I/ρ of infected individuals as a function of ρ for different α on 1000-node BA networks. (b) The epidemic threshold ρ_c as a function of α for different network sizes N. The maximal threshold locates at $\alpha_{\rm opt} \simeq 1.3$, which is indicated by the vertical dotted line. The inset shows $\alpha_{\rm opt}$ as a function of N. All the networks have a fixed average network degree $\langle k\rangle = 6$. (c) The epidemic threshold ρ_c as a function of α for different $\langle k\rangle$. The inset shows $\alpha_{\rm opt}$ as a function of $\langle k\rangle$. $N = 4000$.

value for $\alpha = 1.3$, compared to those for $\alpha = 0, 1.0, 2.0$. This is demonstrated more clearly in Fig. 1(b), where ρ_c is plotted as a function of α for different N. The distinct peak locates at $\alpha_{\rm opt} \simeq 1.3$, which is rather robust to the change of network size N as shown in the inset. In addition, we have also investigated how this phenomenon depends on the average network degree $\langle k\rangle$. As shown in Fig. 1(c), the optimal value $\alpha_{\rm opt}$ also remains nearly constant with varying $\langle k\rangle$ from 4 to 14.

So far we have considered that all species diffuse with the same rate. In the following, we take into account different diffusion rates for different species. For the sake of simplicity, we assume that the infected individuals diffuse with a fixed rate

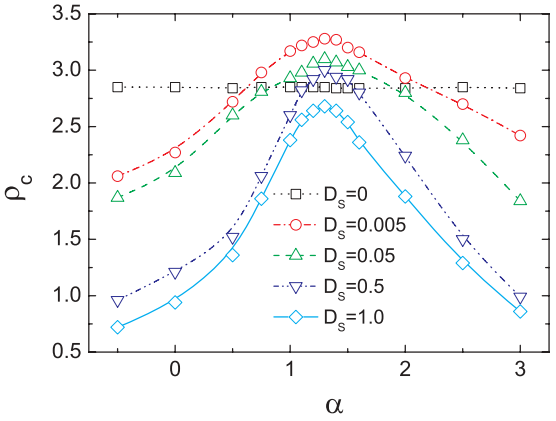

FIG. 2. (Color online) The epidemic threshold ρ_c as a function of α for different diffusion rates D_S. All the networks have fixed $\langle k\rangle = 6$, $N = 1000$, and $\gamma = 3.0$.

$D_I = 1$ and vary the diffusion rate of susceptible ones D_S. The epidemic threshold ρ_c as a function of α is plotted in Fig. 2 for $D_S = 0, 0.005, 0.05, 0.5$, and 1.0. Interestingly, the bell-shape dependence of ρ_c on α always exists for nonzero D_S, with the peak locating at nearly the same optimal value $\alpha_{\rm opt} \simeq 1.3$. The relative height of this peak decreases with increasing D_S, and eventually ρ_c is independent of α for $D_S = 0$.

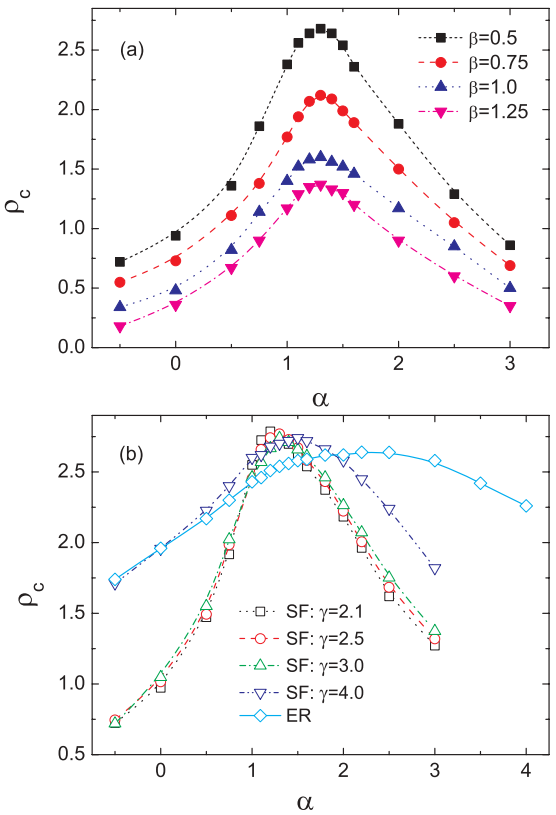

FIG. 3. (Color online) The epidemic threshold ρ_c as a function of α for different infection rates β (a) and for different network topologies (b). The network is of SF type with $\gamma = 3.0$ in panel (a) and the infection rate is $\beta = 0.5$ in panel (b). All the networks have fixed $\langle k\rangle = 6$ and $N = 1000$.

Figure 3(a) shows that ρ_c as a function of α for different infection rates β. It can be found that a maximum ρ_c still shows up at the same $\alpha_{\rm opt}$. Nevertheless, the maximum ρ_c corresponding to $\alpha_{\rm opt}$ does change with β. In addition, we have also considered how the above findings depend on the network topology. To this end, we have performed simulations on SF networks with different exponents γ and on Erdös-Rényi (ER) random networks. The networks are generated according to the Molloy-Reed model [48]: Each node is assigned a random number of stubs k that are drawn from a specified degree distribution, and pairs of unlinked stubs are then randomly joined. This construction eliminates the degree correlations between neighboring nodes. ρ_c as a function of α for different type of networks is shown in Fig. 3(b). It is found that the existence of an maximal ρ_c for optimal α is also robust to the change of network topology. For SF networks, the optimal value of α is always close to 1.3. For ER networks, the $\rho_c \sim \alpha$ curve becomes not so sharp, indicating that ρ_c is not that sensitive to the change of α.

IV. MEAN FIELD ANALYSIS

According to the stochastic simulation schemes, one may write down the following set of dynamic equations at a MF level:

$$\frac{\partial \rho_{I,k}}{\partial t} = \rho_{I,k}(\beta\rho_{S,k} - \mu_k) + D_I\left(k\sum_{k'} p(k'|k)\frac{1}{k'}\rho_{I,k'} - \rho_{I,k}\right), \tag{3a}$$

$$\frac{\partial \rho_{S,k}}{\partial t} = \rho_{I,k}(\mu_k - \beta\rho_{S,k}) + D_S\left(k\sum_{k'} p(k'|k)\frac{1}{k'}\rho_{S,k'} - \rho_{S,k}\right), \tag{3b}$$

where $\rho_{I,k}$ and $\rho_{S,k}$ represent the average densities of infected and susceptible individuals in the nodes with degree k respectively. The first term in the right-hand side of Eq. (3a) accounts for the change of infected individuals due to the reaction (infection and recovery) processes, and the second term accounts for the diffusion of infected individuals into and out of those nodes with degree k. Equation (3b) can be interpreted in a similar manner. $p(k'|k)$ represents the conditional probability that a node of degree k is connected to a node of degree k', which equals to $k'p(k')/\langle k\rangle$ [49,50] for uncorrelated networks.

One notes that a thorough analysis of Eqs. (3) is not easy. For sake of simplicity, here we consider only the case $D_I = D_S = 1$. Then, substituting this into Eqs. (3) and using $\rho_I = \sum_k p(k)\rho_{I,k}$, one obtains

$$\frac{\partial \rho_{I,k}}{\partial t} = \rho_{I,k}(\beta\rho_{S,k} - \mu_k) + \frac{k}{\langle k\rangle}\rho_I - \rho_{I,k}, \tag{4a}$$

$$\frac{\partial \rho_{S,k}}{\partial t} = \rho_{I,k}(\mu_k - \beta\rho_{S,k}) + \frac{k}{\langle k\rangle}\rho_S - \rho_{S,k}. \tag{4b}$$

For $\alpha = 0$ and thus $\mu_k = 1$, it was already shown in the literature that $\rho_c = \frac{\mu}{\beta}\frac{\langle k\rangle^2}{\langle k^2\rangle}$ [25]. For $\alpha \neq 0$, it is hard to get the explicit expression of ρ_c from Eqs. (4) directly. Clearly, Eqs. (4) admit a steady state, which solves $\partial\rho_{I,k}/\partial t =$

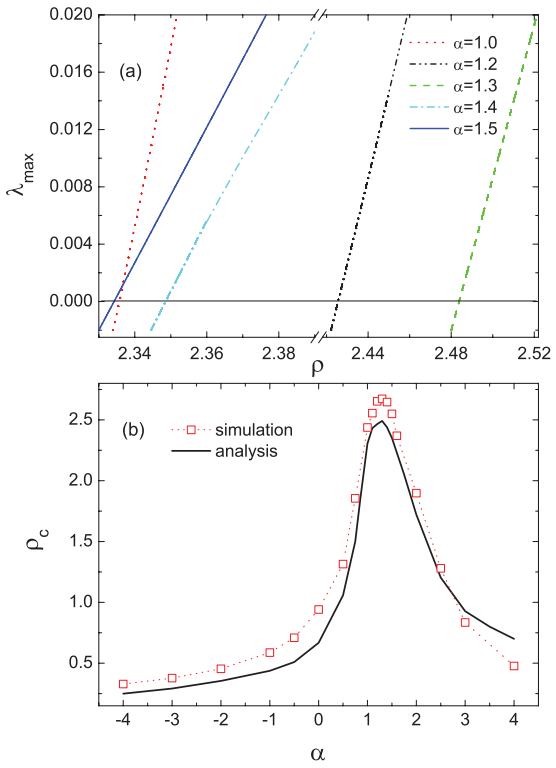

FIG. 4. (Color online) Panels (a) and (b) correspond to the dependence of the largest eigenvalues $\lambda_{\max}$ on ρ for different α and the dependence of ρ_c on α respectively, both on a synthesized 1000-node BA network with $\langle k\rangle = 6$.

$$\partial\rho_{S,k}/\partial t = 0,$$

$$\rho^*_{I,k} = 0, \quad \rho^*_{S,k} = \frac{k}{\langle k\rangle}\rho, \tag{5}$$

which physically corresponds to the disease-free state. Intuitively, this healthy state will lose stability at the critical density ρ_c, above which the steady-state value of $\rho_{I,K}$ cannot be 0 any more. Therefore, one can alternatively perform linear stability analysis of $(\rho^*_{I,k}, \rho^*_{S,k})$ to get ρ_c. Following standard procedures, we need to obtain the Jacobian matrix and calculate the eigenvalues $\{\lambda\}$. The healthy state will lose stability when $\lambda_{\max}$, the largest value of the real part of the eigenvalues, passes through zero from below. Note that explicit expression for $\lambda_{\max}$ is not available, but numerical calculation of it is easy.

Figure 4(a) plots $\lambda_{\max}$ as a function of ρ for several values of α. The value of ρ where $\lambda_{\max} = 0$ corresponds to ρ_c. As expected, ρ_c is largest for $\alpha = 1.3$ compared to those for other α. Figure 4(b) presents ρ_c as a function of α obtained from simulations (symbols) and MF analysis (solid line). Apparently, the MF results are in rather good agreements with the simulation ones.

To get more insights into how the epidemic explosion takes place for different α, we turn to the eigenvector $\mathbf{v} = \{(v_{I,k}, v_{S,k})_{k=1,\ldots}\}$ corresponding to $\lambda_{\max}$ at the onset of the phase transition, that is, $\rho = \rho_c$. The element $v_{I,k}$ of this vector measures the relative amplitude of the fluctuation away from $\rho^*_{I,k} = 0$ for nodes with given degree k. Therefore, the dependence of $v_{I,k}$ on k qualitatively tells us how the epidemic

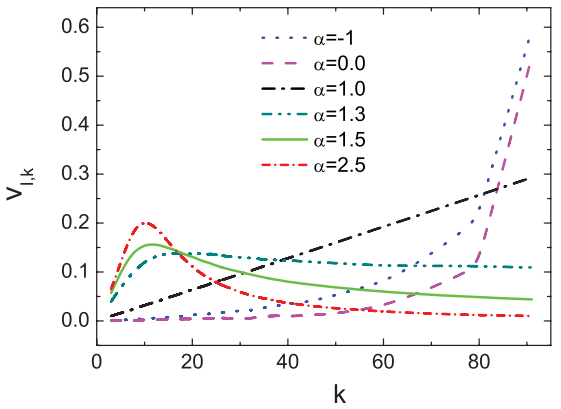

FIG. 5. (Color online) The eigenvectors $\mathbf{v}_{I,k}$, corresponding to the eigenvalue $\lambda_{\max} = 0$, as functions of k for different α. Other parameters are the same as in Fig. 4.

explosion grows from the healthy state. In Fig. 5, we depict the eigenvectors $\mathbf{v}_{I,k}$ as functions of k for different α. Interestingly, we observe that epidemic explosion starts from large-degree nodes for α less than α_{opt}, as shown by the dotted, dashed, and dash dotted lines in Fig. 5, while it is from small-degree nodes for α larger than α_{opt}, as shown by the "solid" and "short dash dotted" lines. For $\alpha \simeq \alpha_{\text{opt}}$, $v_{I,k}$ is not that sensitive on k, indicating a relatively homogenous epidemic explosion.

To reveal the underlying mechanism of the epidemic spreading for different α in more detail, in Fig. 6 we illustrate the time evolution of $\rho_{I,k}/\rho$, the average density of infected

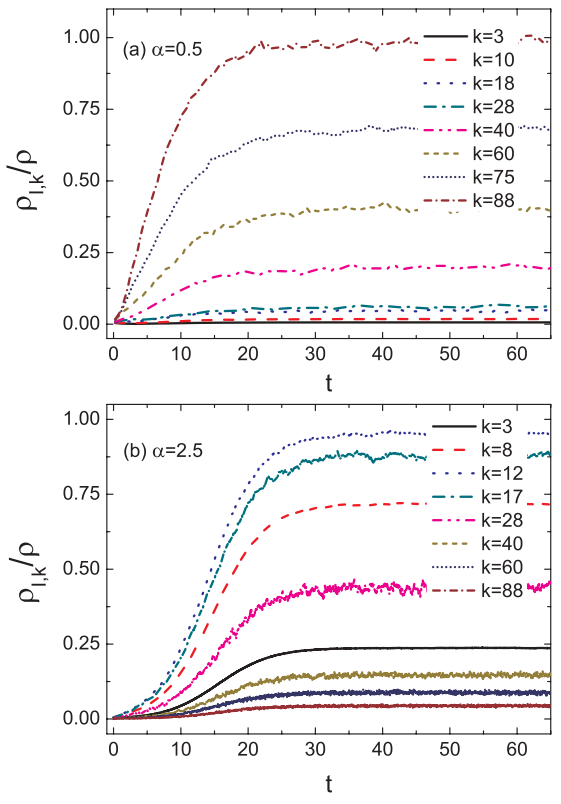

FIG. 6. (Color online) Time evolution of the average density of infected individuals $\rho_{I,k}/\rho$ in the nodes with different degrees for BA model with $N = 1000$ and $\langle k\rangle = 6$. (a) $\alpha = 0.5$, (b) $\alpha = 2.5$.

individuals in the nodes with degree k for two particular values of α, one ($\alpha = 0.5$) less than $\alpha_{\rm opt}$ and the other ($\alpha = 2.5$) larger than it. This can give us more detailed information about how the epidemic outbreak takes place on nodes with different degree k. We find that, for $\alpha = 0.5$, the disease starts to spread from large-degree nodes, such as those with $k = 88$, 75, and 60, as shown by the top three lines in Fig. 6(a); while for $\alpha = 2.5$, the spreading starts from those nodes with relatively small degree, for example, $k = 12$, 17, and 8, as shown in Fig. 6(b). These phenomena indicate that there indeed exist two different epidemic explosion routes for α being less or larger than $\alpha_{\rm opt}$, which are consistent with the analysis associated with the eigenvectors as shown in Fig. 5.

The above different pathways regarding small or large α may be illustrated qualitatively in the following way. Consider that the individuals in a given node are infected at the beginning. These patients will diffuse to neighboring nodes through the links. Certainly, nodes with larger degrees will have more chances to accept these patients. To efficiently suppress the epidemic explosion, the curing rates in such large-degree nodes should be relatively large to compensate these incoming patients via diffusion. Therefore, it is reasonable that μ_k should be an increasing function of k to maintain an effective epidemic control. Intuitively, one may imagine that the most efficient way is to keep linear dependence of μ_k on k (i.e., $\alpha = 1$ in our strategy), considering that every incoming patient via diffusion can be cured on time. However, this is not exactly the case because the reactions inside a node involve nonlinear autocatalytic processes, which makes $\alpha_{\rm opt}$ larger than 1. (Unfortunately, why $\alpha_{\rm opt}$ is so robust to be about 1.3 is still open to us.) If α is too large, which means that the medical resources are biased to large-degree nodes, the patients in small-degree nodes cannot be cured on time. In this case, disease will start to spread from those small-degree nodes. In the contrast case, the disease will start more abruptly from those large-degree nodes since the curing rates there are too smaller than required. These scenario are in agreement with the pictures shown in Figs. 5 and 6.

V. DISCUSSION AND CONCLUSIONS

One should note that the α value cannot be arbitrary for the real world, if we adopt the power-law dependence. Following the recipe of Eq. (2), for a scale-free network with minimum, mean, and maximum degrees respectively of 2, 5, and 100, the recovery rate will range from 0.4 to 20 in the simplest case of linear dependency ($\alpha = 1$). This large difference is to some extent not reasonable, which implies that the optimal control with $\alpha = 1.3$ is hard to be realized practically. Nevertheless, as a model study, we can just change α as we want to see what we can find. If, for instance, we tune α to a reasonable nonzero value, say $\alpha = 0.5$, the ratio of the maximal and minimal μ would be about 10 for a network with k ranging from 1 to 100, which can also lead to a much better epidemic control ($\rho_c = 1.37$) than previous case of $\alpha = 0$ ($\rho_c = 0.95$). Therefore, our work has indeed provided an efficient strategy to suppress the epidemic explosion.

In summary, we have studied a variant of SIS model defined on scale-free metapopulation networks, wherein the curing rate in a node with degree k is proportional to k^α. By detailed numerical simulations, we show that the epidemic threshold reaches a maximum value when α is tuned to be $\alpha_{\rm opt} \simeq 1.3$, which corresponds to an optimal control strategy to suppress epidemic explosion and is robust to the change of network size or average degree. We have also performed a mean field analysis to further elucidate this strategy and unravel the distinct pathways to epidemic spreading for α larger or less than $\alpha_{\rm opt}$. Our findings suggest that a proper allocation of medical resources can best suppress the epidemic explosion, which could be of great importance in practical epidemic control.

ACKNOWLEDGMENTS

This work was supported by the National Natural Science Foundation of China (Grants No. 21125313, No. 20933006, No. 91027012, and No. 11205002). C.S.S. was also supported by the Key Scientific Research Fund of Anhui Provincial Education Department (Grant No. KJ2012A189).

[1] R. Albert and A.-L. Barabási, Rev. Mod. Phys. **74**, 47 (2002).
[2] S. N. Dorogovtsev and J. F. F. Mendes, Adv. Phys. **51**, 1079 (2002).
[3] M. E. J. Newman, SIAM Review **45**, 167 (2003).
[4] S. Boccaletti, V. Latora, Y. Moreno, M. Chavez, and D.-U. Hwang, Phys. Rep. **424**, 175 (2006).
[5] A. Arenas, A. Díaz-Guilera, J. Kurths, Y. Moreno, and C. Zhou, Phys. Rep. **469**, 93 (2008).
[6] S. N. Dorogovtsev, A. V. Goltsev, and J. F. F. Mendes, Rev. Mod. Phys. **80**, 1275 (2008).
[7] R. Pastor-Satorras and A. Vespignani, Phys. Rev. Lett. **86**, 3200 (2001).
[8] R. Pastor-Satorras and A. Vespignani, Phys. Rev. E **63**, 066117 (2001).
[9] M. Boguñá and R. Pastor-Satorras, Phys. Rev. E **66**, 047104 (2002).
[10] M. Boguñá, R. Pastor-Satorras, and A. Vespignani, Phys. Rev. Lett. **90**, 028701 (2003).
[11] M. Barthélemy, A. Barrat, R. Pastor-Satorras, and A. Vespignani, Phys. Rev. Lett. **92**, 178701 (2004).
[12] R. M. May and A. L. Lloyd, Phys. Rev. E **64**, 066112 (2001).
[13] A. L. Lloyd and R. M. May, Science **292**, 1316 (2001).
[14] Y. Moreno, R. Pastor-Satorras, and A. Vespignani, Eur. Phys. J. B **26**, 521 (2002).
[15] Y. Moreno, J. B. Gómez, and A. F. Pacheco, Phys. Rev. E **68**, 035103 (2003).
[16] J. Joo and J. L. Lebowitz, Phys. Rev. E **69**, 066105 (2004).
[17] R. Olinky and L. Stone, Phys. Rev. E **70**, 030902(R) (2004).
[18] Z. Liu and B. Hu, Europhys. Lett. **72**, 315 (2005).
[19] G. Yan, Z.-Q. Fu, J. Ren, and W.-X. Wang, Phys. Rev. E **75**, 016108 (2007).
[20] C. Castellano and R. Pastor-Satorras, Phys. Rev. Lett. **105**, 218701 (2010).
[21] M. Kitsak, L. K. Gallos, S. Havlin, F. Liljeros, L. Muchnik, H. E. Stanley, and H. A. Makse, Nat. Phys. **8**, 888 (2010).
[22] N. Masuda, New J. Phys. **12**, 093009 (2010).

[23] F. M. Neri, A. Bates, W. S. Füchtbauer, F. J. Pérez-Reche, S. N. Taraskin, W. Otten, D. J. Bailey, and C. A. Gilligan, PLoS Comput. Biol. **7**, e1002174 (2011).
[24] V. Belik, T. Geisel, and D. Brockmann, Phys. Rev. X **1**, 011001 (2011).
[25] V. Colizza, R. Pastor-Satorras, and A. Vespignani, Nat. Phys. **3**, 276 (2007).
[26] V. Colizza and A. Vespignani, Phys. Rev. Lett. **99**, 148701 (2007).
[27] V. Colizza and A. Vespignani, J. Theor. Biol. **251**, 450 (2008).
[28] A. Gautreau, A. Barrat, and M. Barthélemy, J. Theor. Biol. **251**, 509 (2008).
[29] A. Baronchelli, M. Catanzaro, and R. Pastor-Satorras, Phys. Rev. E **78**, 016111 (2008).
[30] P. Wang, M. C. González, C. A. Hidalgo, and A.-L. Barabási, Science **324**, 1071 (2009).
[31] S. Kondo and T. Miura, Science **329**, 1616 (2010).
[32] A. Nakamasu, G. Takahashi, A. Kanbe, and S. Kondo, Proc. Natl. Acad. Sci. USA **106**, 8429 (2009).
[33] L. Lizana, Z. Konkoli, B. Bauer, A. Jesorka, and O. Orwar, Annu. Rev. Phys. Chem. **60**, 449 (2009).
[34] B. A. Grzybowski, *Chemistry in Motion: Reaction-Diffusion Systems for Micro- and Nanotechnology* (Wiley, Chichester, 2009).
[35] Q. Xuan, F. Du, T.-J. Wu, and G. Chen, Phys. Rev. E **82**, 046116 (2010).
[36] D. Balcan and A. Vespignani, J. Theor. Biol. **293**, 87 (2012).
[37] M. Barthélemy, Phys. Rep. **499**, 1 (2011).
[38] V. Nicosia, F. Bagnoli, and V. Latora, Europhys. Lett. **94**, 68009 (2011).
[39] A. Moilanen, K. Wilson, and H. Possingham, *Spatial Conservation Prioritization* (Oxford University Press, London, 2009).
[40] D. Balcan and A. Vespignani, Nat. Phys. **7**, 581 (2011).
[41] A. Vespignani, Nat. Phys. **8**, 32 (2012).
[42] H. Nakao and A. S. Mikhailov, Nat. Phys. **6**, 544 (2010).
[43] D. J. Daley and J. Gani, *Epidemic Modelling* (Cambridge University Press, Cambridge, 1999).
[44] H. W. Hethcote, SIAM Rev. **42**, 599 (2000).
[45] J. D. Murray, *Mathematical Biology* (Springer-Verlag, Berlin, 2002).
[46] A.-L. Barabási and R. Albert, Science **286**, 509 (1999).
[47] M. E. J. Newman, Phys. Rev. E **66**, 016128 (2002).
[48] M. Molloy and B. Reed, Random Structures Algorithms **6**, 161 (1995).
[49] R. Pastor-Satorras, A. Vázquez, and A. Vespignani, Phys. Rev. Lett. **87**, 258701 (2001).
[50] S. N. Dorogovtsev and J. F. F. Mendes, *Evolution of Networks: From Biological Nets to the Internet and WWW* (Oxford University Press, Oxford, 2003).